Time-Synchronized Control for Disturbed Systems

Dongyu Li, *Member, IEEE*, Keng Peng Tee, *Member, IEEE*, Lihua Xie, *Fellow, IEEE*, and Haoyong Yu, *Senior Member, IEEE*

***Abstract*—Finite-time control is concerned with steering a system state to the origin before a certain settling-time limit, ignoring any consideration of when each state element converges relative to the others. In this article, a control problem called *time-synchronized control* is investigated, where all the system state elements have to converge to the origin *at the same time*. To facilitate this problem formulation, we introduce the notion of *time-synchronized stability* together with sufficient Lyapunov conditions. Based on these, the analytical solution of a time-synchronized stable system is obtained and discussed, explicitly offering a quantitative method to preview and predesign the control system performance *in prior*. Following these results, a robust time-synchronized control law is designed for multivariable systems under external disturbances and model uncertainties. Finally, comparative numerical simulations between time-synchronized control and finite/fixed/prescribed-time control are conducted to showcase the time-synchronized features attained.**

***Index Terms*—Disturbance rejection, finite-time control, time-synchronized convergence.**

I. Introduction

FINITE-TIME control has grown in relevance to the research community due to its high-precision performance. Its applications include robot trajectory tracking [1]–[5], satellite attitude stabilization [6]–[8], state estimation of dynamical systems [9]–[12], networked system control [13]–[19], fuzzy system control [20]–[22], etc.

Finite-time control guarantees that all the elements of a system state converge to the origin within bounded settling time, which is related to the initial state [23], [24]. Furthermore, fixed-time stability is developed in [25] and [26] to yield an upper bound of the settling time regardless of the initial conditions. Based on the time-varying high-gain feedback, prescribed-time control is capable of likewise achieving finite/fixed-time convergence with a predefined settling time [27], [28]. Although finite/fixed-time stability offers superior advantages to a control system, unfortunately, standalone finite/fixed-time convergence is not sufficient for some applications, in which the control system (with diversified subsystems) is expected to accomplish multiple actions *time synchronously*, that is, the state elements are required to converge to desired values *at the same time*. For example, the finger joints of a robotic hand are required to reach the desired angles simultaneously so as to grasp the surface or the contour of an object firmly, failing which the object is likely to slip or escape. Moreover, in cooperative transport/monitoring, cooperative attack, or leader–follower consensus, multiagent systems are to reach the desired location synchronously [29]–[32].

In the authors' recent result [33], inspired by the multivariable sliding-mode approach [34]–[39], time-synchronized control and its stability analysis are proposed to force all the state elements of a given system to reach the equilibrium at the same time. It shows that "Finite-Time Stability" $+$ "Ratio Persistence" $\Rightarrow$ "Time-Synchronized Stability" (ratio persistence implies that the ratio of each pair of the state elements is *time invariant* in forward time). Fixed-time-synchronized stability is also investigated as a special type of time-synchronized stability where the upper bound of the synchronized settling time is independent of any initial state. Certain types of elegant control design in the literature appear to achieve also time-synchronized convergence if the target system meets the sufficient conditions of time-synchronized stability introduced in [33]. Furthermore, based on time-synchronized stability, time-synchronized consensus control of multiagent systems is addressed in [40], where all the state elements of all the agents achieve an agreement time synchronously.

Despite the establishment of time-synchronized stability in [33] and [40], the control design, therein, can only be implemented under the assumptions that the system model is accurate and there exist no external disturbances. It inevitably limits possible practical implementations of this control design. In addition, the analytical solutions of (fixed-) time-synchronized stable systems are likewise not investigated.

Based on the discussion above, we are interested in exploring the time-synchronized control problem, taking into consideration model uncertainties and external disturbances, for a class of multivariable systems. On the other hand, under certain conditions, we study the analytical solutions of time-synchronized stable systems, which hold various advantages in

Manuscript received May 20, 2020; revised September 19, 2020 and January 4, 2021; accepted January 13, 2021. This work was supported in part by the Science and Engineering Research Council, Agency of Science, Technology and Research, Singapore, through the National Robotics Program under Grant 192 25 00054, and in part by the Natural Science Foundation of Jiangsu Province under Grant BK20200239. This article was recommended by Associate Editor Q. Liu. *(Corresponding author: Haoyong Yu.)*

Dongyu Li is with the School of Cyber Science and Technology, Beihang University, Beijing 100191, China, and also with the Department of Biomedical Engineering, National University of Singapore, Singapore 117583.

Keng Peng Tee is with the Institute for Infocomm Research, A*STAR, Singapore 138632.

Lihua Xie is with the School of Electrical and Electronic Engineering, Nanyang Technological University, Singapore 639798.

Haoyong Yu is with the Department of Biomedical Engineering, National University of Singapore, Singapore 117583 (e-mail: bieyhy@nus.edu.sg).

control system design, for example, being capable of explicitly and quantitatively previewing and manipulating the system performance in advance.

The contributions of this article are as follows. First, we rewrite the Lyapunov-like sufficient conditions of time-synchronized stability, in which under some additional constraints, the explicit synchronized settling time and the analytical solution of a time-synchronized stable system are provided. The specific importance of the analytical solution lies in that the system state and its tendency at each time instant are precisely obtained in advance, which also provides a quantitative indicator to predesign and adjust the control parameters of the system design to achieve desired performance. Moreover, fixed-time-synchronized stability and its corresponding Lyapunov-based analysis are discussed. Based on a modified fixed-time-synchronized stability formulation, the analytical solution of a fixed-time-synchronized system is then investigated to determine the accurate settling time of a fixed-time stable system.

Second, it is noteworthy that the time-synchronized control design in consideration of unknown disturbances and uncertainties has not been touched on. Thus, we aim at designing a control law for a class of disturbed affine systems to achieve time-synchronized convergence. Inspired by the super-twisting approach in [41] and [42], we propose a robust time-synchronized control law integrated with a multivariable disturbance observer. The observer is able to precisely estimate the unknown system dynamics in finite time. Based on the proposed relevant Lyapunov theorem, the time-synchronized stability of the disturbed system is rigorously proved, where the analytical solution of the closed-loop system is presented in addition. The extensions to time-synchronized control of other system dynamics are provided.

The remainder of this article is organized as follows. In Section II, some technical preliminaries are introduced. In Section III, time-synchronized stability and the related Lyapunov conditions are described, based on which time-synchronized controllers (TSCs) are designed. In Section IV, simulations are presented to show the merit of the proposed approach, before conclusions are drawn in Section V.

Notations: Let $\mathbb{R}$ denote the set of real numbers, and $I_n \in \mathbb{R}^{n\times n}$ denote an n-dimensional identity matrix. Let $\lambda_{\max}(\cdot)$ and $\lambda_{\min}(\cdot)$ denote the maximum and minimum eigenvalues of a matrix, respectively. Denote $\|\cdot\|$ as the L_2-norm of a vector, and $\det(\cdot)$ as the determinant of a matrix.

II. Preliminaries

We consider the following system dynamics:

$$\dot{x} = f(x), \quad f(0) = 0, \quad x(0) = x_0 \tag{1}$$

where $x = [x_1, \ldots, x_n]^T \in \mathbb{R}^n$, and with respect to an open neighborhood $\mathcal{D}_0 \subseteq \mathbb{R}^n$ of the origin, $f : \mathcal{D}_0 \to \mathbb{R}^n$ is continuous. We assume that the system (1) has a unique solution for all initial conditions in forward time. Next, the following well-established results are introduced.

Definition 1 [24]: The equilibrium of system (1) is finite-time stable if for an open neighborhood $\mathcal{N}_0 \subseteq \mathcal{D}_0$ of the origin $\forall x_0 \in \mathcal{N}_0\backslash\{0\}$, $x(t) \in \mathcal{N}_0\backslash\{0\}$, $\lim_{t\to T(x_0)} x(t) = 0$, where $T(x_0)$ is the settling time. The equilibrium is globally finite-time stable if it is finite-time stable with $\mathcal{N}_0 = \mathcal{D}_0 = \mathbb{R}^n$.

Lemma 1 [24]: Considering a Lyapunov function $V(x)$, for any real numbers $c > 0$ and $\alpha \in (0, 1)$, the origin of the system (1) is finite-time stable if $\dot{V}(x) + cV^{\alpha(x)} \leq 0$, where the settling time is estimated by $T(x_0) \leq (V^{1-\alpha}(x_0)/c(1-\alpha))$.

Definition 2 [25]: The equilibrium of the system (1) is fixed-time stable if it is globally finite-time stable with bounded settling time $T(x_0)$, where the bound is independent of any initial system state, that is, for $\forall x_0$, we have $T(x_0) < T_m$, where T_m is a positive constant.

Lemma 2 [25]: The equilibrium of the system (1) is fixed-time stable, if there exists a Lyapunov function $V(x)$ such that along the state trajectory of (1), we have

$$\dot{V}(x) \leq -\big(\alpha V^p(x) + \beta V^g(x)\big)^\chi \tag{2}$$

where α, β, p, g, and χ are positive constants, with $p\chi < 1$ and $g\chi > 1$. The settling time $T(x_0)$ is bounded as $T(x_0) \leq (1/\alpha^\chi(1-p\chi)) + (1/\beta^\chi(g\chi-1))$.

III. Main Results

In this section, the Lyapunov analysis of (fixed-) time-synchronized stability is proposed where the analytical solutions of (fixed-) time-synchronized stable systems are derived under certain conditions. A TSC is then designed for a class of multivariable systems under unknown disturbances or system uncertainties than can lumped into disturbances.

A. Time-Synchronized Stability

We introduce time-synchronized stability as follows.

Definition 3 Time-Synchronized Stability [33]: The equilibrium of the system (1) is *time-synchronized stable* if:

1) it is finite-time stable;
2) for an open neighborhood $\mathcal{N}_0 \subseteq \mathcal{D}_0$ of the origin, there exists a function $T : \mathcal{N}_0\backslash\{0\} \to (0,\infty)$, called the *synchronized settling-time function*, such that for $\forall x_0 \in \mathcal{N}_0\backslash\{0\}$ and $i \in \{1, 2, \ldots, n\}$, we have $x(t) \in \mathcal{N}_0$, $\forall t \in [0,\infty)$, and for $x_i(0) \neq 0$,

$$x_i(t) \neq 0, \quad \lim_{t\uparrow T(x_0)} x_i(t) = 0 \quad \forall t \in [0, T(x_0)) \tag{3}$$

where $T(x_0)$ is the *synchronized settling time*.

The equilibrium is globally time-synchronized stable if it is time-synchronized stable with $\mathcal{N}_0 = \mathcal{D}_0 = \mathbb{R}^n$.

Time-synchronized stability is a more strict, special form of finite-time stability. Specifically, finite-time stability allows some of the state elements to arrive at the origin before $T(x_0)$ as long as the remaining state elements converge to zero as $t \to T(x_0)$, while time-synchronized stability requires all state elements x_i to arrive at the origin at the same time $T(x_0)$.

In the sequel, we introduce an *indirect* method to achieve time-synchronized stability, which involves proving that system (1) is finite-time stable, and during convergence, the ratio of each pair of state elements is always constant. For convenience, the following notion of *ratio persistence* is recalled.

Definition 4 (Ratio Persistence [33]): The closed-loop state x of the system (1) is *ratio persistent* if for $x \neq 0$, we have

$$\frac{x}{\|x\|} = \zeta \frac{f(x)}{\|f(x)\|} \tag{4}$$

where ζ is the *direction of ratio persistence*, which can be either 1 or -1.

In fact, various known control methods in the literature (e.g., [35], [36], and many others using the unit-vector-based technique [34]) can allow a given system to meet this condition. Next, the following property of ratio persistence is given.

Lemma 3: If the system state x is ratio persistent, for $\forall x_i(t)$, $x_j(t) \neq 0,\ i, j \in \{1, 2, \ldots, n\}$, $i \neq j$, we have

$$\frac{x_i(t)}{x_j(t)} = c_{ij} \tag{6}$$

where $c_{ij} = x_i(0)/x_j(0)$ is a nonzero constant.

Proof: The proof readily follows from (20), (21) in [33]. ■

A ratio persistent trajectory of the state x is the shortest path between any initial state and the equilibrium if x denotes the system position in $\mathbb{R}^2$ or $\mathbb{R}^3$ Euclidean space, which is optimal in terms of its travel length.

Given the definitions of time-synchronized stability and ratio persistence, the following Lyapunov-like result is next introduced from [33], that is, "Finite-Time Stable" + "Ratio Persistent" ⇒ "Time-Synchronized Stable."

Lemma 4: Considering a Lyapunov function $V(x)$, the origin of system (1) is TSS, with the synchronized settling time $T(x_0) \leq (V^{1-\alpha}(x_0)/c(1-\alpha))$, if the following conditions hold.

1) There exist constants $c > 0$ and $\alpha \in (0, 1)$, such that $\dot{V}(x) + cV^{\alpha}(x) \leq 0$.
2) The state x is ratio persistent.

For example, we consider an autonomous system in $\mathbb{R}^n$

$$\dot{x} = -\mathrm{sig}_{\mathrm{n}}^{\alpha}(x) \tag{7}$$

where $\alpha \in (0, 1)$ and the sign function $\mathrm{sig}_{\mathrm{n}}^{\alpha}(x)$ is defined as follows:

$$\mathrm{sig}_{\mathrm{n}}^{\alpha}(x) = \|x\|^{\alpha}\mathrm{sign}_{\mathrm{n}}(x) \tag{8}$$

$$\mathrm{sign}_{\mathrm{n}}(x) \triangleq \begin{cases} \dfrac{x}{\|x\|}, & x \neq 0 \\ 0, & x = 0. \end{cases} \tag{9}$$

By using Lemma 1, considering a Lyapunov function $V = x^T x$, the solution of the system (7) can be proved to be finite-time stable with settling time

$$T(x_0) = \frac{\|x_0\|^{1-\alpha}}{1-\alpha}. \tag{10}$$

Next, according to Definition 4, one can easily verify the ratio persistent property of the system (7). Evidently, time-synchronized stability is achieved from Lemma 4.

Note that the system (7) is continuous and locally Lipschitz except at the origin. We can directly obtain the analytical solution of the system for any initial condition x_0 in $\mathbb{R}^n \backslash \{0\}$, which will explicitly show how and when the system state converges. The solution takes the following form:

$$x = \left(\|x_0\|^{1-\alpha} - (1-\alpha)t\right)^{\frac{1}{1-\alpha}} \frac{x_0}{\|x_0\|} \tag{11}$$

when $t < \|x_0\|^{1-\alpha}/(1-\alpha)$, and $x = 0$ when $t \geq \|x_0\|^{1-\alpha}/(1-\alpha)$. This solution is clearly ratio persistent. Moreover, it infers that all elements of $x(t)$ converge to the origin at the same time $t = \|x_0\|^{1-\alpha}/(1-\alpha)$, which is in line with (10).

Based on the above discussion, we are now ready to provide a Lyapunov-like result of time-synchronized stability based on Lemma 4, where under some additional constraints, the analytical solution of system (1) and its synchronized settling time are derived.

Theorem 1: Considering a Lyapunov function $V(x)$, the origin of the system (1) is time-synchronized stable, with the synchronized settling time

$$T(x_0) \leq \frac{V^{1-\alpha}(x_0)}{c(1-\alpha)} \tag{12}$$

if the following conditions hold.

1) There exist constants $c > 0$ and $\alpha \in (0, 1)$ such that
$$\dot{V}(x) + cV^{\alpha}(x) \leq 0. \tag{13}$$
2) The state x is ratio persistent.

As a special case, if for $k > 0$

$$V(x) = kx^T x,\ \dot{V}(x) + cV^{\alpha}(x) = 0 \tag{14}$$

the system (1) has an explicit synchronized settling time

$$T(x_0) = \frac{V^{1-\alpha}(x_0)}{c(1-\alpha)} \tag{15}$$

and its analytical solution takes the form [see (5)].

Proof: Following Lemma 4, we know that in the case of an arbitrary $V(x)$ with $V(x) + cV^{\alpha}(x) \leq 0$, the closed-loop system is time-synchronized stable.

Next, consider the case of $V(x) = kx^T x$ with $\dot{V}(x) + cV^{\alpha}(x) = 0$.

By (14) and Lemma 1, the system (1) is finite-time stable with the settling time

$$T(x_0) = \frac{V^{1-\alpha}(x_0)}{c(1-\alpha)} \tag{16}$$

after which, the state will stay at the origin.

$$x = \begin{cases} \left(\|x_0\|^{2-2\alpha} - c(1-\alpha)k^{\alpha-1}t\right)^{\frac{1}{2-2\alpha}} \dfrac{x_0}{\|x_0\|}, & t < T(x_0),\ \ x_0 \neq 0 \\ 0, & t \geq T(x_0),\ \ x_0 \neq 0 \\ 0, & t \geq 0, \qquad\ \ x_0 = 0 \end{cases} \tag{5}$$

In the following, by analyzing the case of $x(t) \neq 0$, $t < T(x_0)$, we will prove that all the state elements reach the origin synchronously, and derive the analytical solution of the closed-loop system (1).

Since $V(x) = kx^T x$, we have

$$\dot{V}(x) = 2kx^T \dot{x}. \tag{17}$$

Note that according to (14), we can obtain

$$\dot{V}(x) = -cV^{\alpha(x)} = -ck^{\alpha} \|x\|^{2\alpha} \tag{18}$$
$$= -ck^{\alpha} x^T \operatorname{sig}_{\mathrm{n}}^{2\alpha-1}(x). \tag{19}$$

Substituting (17) into (18), we can further obtain

$$2kx^T \dot{x} = -ck^{\alpha} x^T \operatorname{sig}_{\mathrm{n}}^{2\alpha-1}(x). \tag{20}$$

Since the system state x is ratio persistent, for $x \neq 0$, we have

$$\dot{x} = \kappa(x)x \tag{21}$$

where the function $\kappa: \mathcal{N}_0 \backslash \{0\} \to \mathbb{R}$ is defined as

$$\kappa(x) = \zeta^{-1} \frac{\|f(x)\|}{\|x\|}. \tag{22}$$

From (4), we know that $\kappa(x) \neq 0$ when $x \neq 0$.

Taking (21) into (20), it yields for $x \neq 0$

$$\kappa(x) = -\frac{ck^{\alpha-1}}{2\|x\|^{2-2\alpha}}. \tag{23}$$

Therefore, we can obtain that for $x \neq 0$

$$\dot{x} = \kappa(x)x = -\frac{c}{2}k^{\alpha-1}\frac{x}{\|x\|^{2-2\alpha}}. \tag{24}$$

Again, as the system state x is ratio persistent, for $x \neq 0$, we know $x = \lambda e$, where $\lambda(t) \in \mathbb{R}$ is an unknown scalar variable to be solved and $e \in \mathbb{R}^n$ is a unit vector defined as $e = x_0/\|x_0\|$.

Then, (24) leads to

$$\dot{\lambda} = -\frac{c}{2}k^{\alpha-1}\frac{\lambda}{|\lambda|^{2-2\alpha}}. \tag{25}$$

Define $\lambda_0 = \lambda(0)$. The closed-form solution is given by

$$\lambda = \left(|\lambda_0|^{2-2\alpha} - c(1-\alpha)k^{\alpha-1}t\right)^{\frac{1}{2-2\alpha}}. \tag{26}$$

Based on (26), we obtain an expression for x as follows:

$$x = \left(\|x_0\|^{2-2\alpha} - c(1-\alpha)k^{\alpha-1}t\right)^{\frac{1}{2-2\alpha}} \frac{x_0}{\|x_0\|} \tag{27}$$

where $x_0 \neq 0$.

Due to the continuity of the system (1), the solution (27) shows that the all the state elements $x_i(t)$ will arrive at the origin when

$$t \to \frac{\|x_0\|^{2-2\alpha}}{c(1-\alpha)k^{\alpha-1}}. \tag{28}$$

One can also verify from (16) that

$$T(x_0) = \frac{\|x_0\|^{2-2\alpha}}{c(1-\alpha)k^{\alpha-1}} \tag{29}$$

which is in line with (28).

According to (27), the analytical solution of the closed-loop system state x takes the form as in (5), which infers that all the state elements $x_i(t)$ converge to the origin at the same time $T(x_0)$. The solution (5) meets the requirements in Definition 3 of time-synchronized stability, which completes the proof here. ■

Remark 1: Note that the Lyapunov function of the special case in Theorem 1 is restricted to a quadratic form $V(x) = kx^T x$. However, it still represents a class of commonly used Lyapunov function candidates. More importantly, this special case allows us to obtain the analytical solution of the closed-loop system as well as the synchronized settling time, which are important for quantifying system performance and tuning/optimizing design parameters.

Remark 2: Ratio persistence is a vital condition of Theorem 1, because if we only have the equality (14) without ratio persistence of state x, the conclusion of time-synchronized stability no longer holds. Specifically, one cannot obtain (24) from (20) due to the lack of ratio persistence, since

$$x^T\left(2k\dot{x} + ck^{\alpha}\operatorname{sig}_{\mathrm{n}}^{2\alpha-1}(x)\right) = 0 \tag{30}$$

does not necessarily mean that

$$\dot{x} = -\frac{c}{2}k^{\alpha-1}\operatorname{sig}_{\mathrm{n}}^{2\alpha-1}(x). \tag{31}$$

Theorem 1 can be extended to the case of fixed-time stability, where all the ratio persistent state elements converge to the origin at the same time, with the synchronized settling time disregard for the initial state.

Definition 5 Fixed-Time-Synchronized Stability [33]: The equilibrium of the system (1) is *fixed-time-synchronized stable* if:

1) it is globally time-synchronized stable in the sense of Definition 3;
2) the upper bound of the synchronized settling time $T(x_0)$ is independent of any initial system state, that is, for $\forall x_0$, we have $T(x_0) \leq T_m$, where T_m is a positive constant.

We recall the sufficient condition of fixed-time-synchronized stability in [33].

Lemma 5 [33]: Considering a Lyapunov function $V(x)$, the origin of the system (1) is fixed-time-synchronized stable, with the synchronized settling time $T(x_0) \leq (1/\alpha^{\chi}(1 - p\chi)) + (1/\beta^{k}(g\chi - 1))$, if the following conditions hold.

1) There exist positive constants α, β, p, g, and χ satisfying $p\chi < 1$ and $g\chi > 1$, such that $\dot{V}(x) \leq -(\alpha V^{p}(x) + \beta V^{g}(x))^{\chi}$.
2) The state x is ratio persistent.

Note that it is generally not easy to obtain the analytical solution of a fixed-time (-synchronized) stable system as Theorem 1 does. For example, given a Lyapunov function $V(x) = kx^T x$, where k is a positive constant, if there exist positive constants α, β, p, and g satisfying $p < 1$ and $g > 1$, such that

$$\dot{V}(x) = -\alpha V^{p}(x) - \beta V^{g}(x) \tag{32}$$

from Lemma 2 (see [25] for more details), the settling time will still be estimated by

$$T(x_0) \le \frac{1}{\alpha(1-p)} + \frac{1}{\beta(g-1)} \tag{33}$$

rather than a determinate value

$$T(x_0) = \frac{1}{\alpha(1-p)} + \frac{1}{\beta(g-1)}. \tag{34}$$

Based on (33), we cannot derive the analytical solution of the closed-loop system (1) as Theorem 1 does.

Despite the difficulty, we can still explore the analytical solution of a fixed-time synchronized stable system based on a modified sufficient condition of fixed-time stability. First, Lemma 2 is rewritten as follows.

Lemma 6: The equilibrium of the system (1) is fixed-time stable, if there exists a Lyapunov function $V(x)$ such that along the state trajectory of (1)

$$\dot{V}(x) \le \begin{cases} -cV^g(x), & \text{if } V(x) > 1 \\ -cV^p(x), & \text{if } V(x) \le 1 \end{cases} \tag{35}$$

where c, p, and g are positive constants, satisfying $p < 1$ and $g > 1$. The settling time $T(x_0)$ is bounded as

$$T(x_0) \le \frac{1}{c(1-p)} + \frac{1}{c(g-1)}. \tag{36}$$

Proof: The proof can be given based on the proof of [25, Lemma 1]. ■

Next, readily following from Lemma 6, the analytical solution of a fixed-time-synchronized system is inspected.

Theorem 2: Considering a Lyapunov function $V(x) = kx^T x$ where $k > 0$, if the state x is ratio persistent and the following equality holds:

$$\dot{V}(x) = \begin{cases} -cV^g(x), & \text{if } V(x) > 1 \\ -cV^p(x), & \text{if } V(x) \le 1 \end{cases} \tag{37}$$

where constants $c > 0$, $g > 1$ and $p \in (0, 1)$, the origin of the system (1) is fixed-time-synchronized stable. The system (1) has an explicit synchronized settling time

$$T(x_0) = \begin{cases} \dfrac{1 - V^{1-g}(x_0)}{c(g-1)} + \dfrac{1}{c(1-p)}, & \text{if } V(x_0) > 1 \\ \dfrac{V^{1-p}(x_0)}{c(1-p)}, & \text{if } V(x_0) \le 1. \end{cases} \tag{38}$$

The analytical solution of the closed-loop system (1) takes the form: 1) in the case of $V(x_0) > 1$

$$x = \begin{cases} \left(\|x_0\|^{2-2g} - \vartheta_g t\right)^{\frac{1}{2-2g}} \dfrac{x_0}{\|x_0\|}, & \text{if } t < T_0 \\ \left(k^{p-1} - \vartheta_p (t - T_1)\right)^{\frac{1}{2-2p}} \dfrac{x_0}{\|x_0\|}, & \text{if } t \ge T_0 \end{cases} \tag{39}$$

and 2) in the case of $V(x_0) \le 1$

$$x = \left(\|x_0\|^{2-2p} - \vartheta_p t\right)^{\frac{1}{2-2p}} \frac{x_0}{\|x_0\|} \tag{40}$$

where $T_0 = (1 - V^{1-g}(x_0))/(c(g-1))$, $\vartheta_p = c(1-p)k^{p-1}$, and $\vartheta_g = c(1-g)k^{g-1}$. In addition, for $\forall x_0 \in \mathbb{R}^n$, the synchronized settling time is uniformly bounded by

$$T(x_0) \le \frac{1}{c(1-p)} + \frac{1}{c(g-1)}. \tag{41}$$

Proof: The proof is given in two cases.

Case 1 ($V(x_0) > 1$): Considering $V(x) > 1$, we have $\|x\| > \sqrt{k}/k$. Since the state x is ratio persistent and $\dot{V}(x) = -cV^g(x)$, according to Theorem 1, the analytical solution takes the form

$$x = \left(\|x_0\|^{2-2g} - \vartheta_g t\right)^{\frac{1}{2-2g}} \frac{x_0}{\|x_0\|}. \tag{42}$$

Following the proof of Theorem 1, the derivative of the state x is derived

$$\dot{x} = -\frac{c}{2} k^{g-1} \frac{x}{\|x\|^{2-2g}}. \tag{43}$$

Based on the solution (42), the settling time for $\|x\| \to \sqrt{k}/k$ can be calculated

$$T_1 = \frac{1}{c(g-1)} \left(1 - \frac{1}{\|x_0\|^{2g-2} k^{g-1}}\right). \tag{44}$$

Considering $V(x) \le 1$, we have $\|x\| \le \sqrt{k}/k$. From Theorem 1, it reads

$$x = \left(k^{p-1} - \vartheta_p (t + T_1)\right)^{\frac{1}{2-2p}} \frac{x_0}{\|x_0\|}. \tag{45}$$

Similarly, we can obtain

$$\dot{x} = -\frac{c}{2} k^{p-1} \frac{x}{\|x\|^{2-2p}}. \tag{46}$$

It is worth noting that when $\|x\| = \sqrt{k}/k$, (43) and (46) are equal, which guarantees the continuity of the derivative of the state x.

The corresponding settling time is derived from (45)

$$T_2 = \frac{1}{c(1-p)}. \tag{47}$$

The total synchronized settling time is obtained

$$T = T_1 + T_2 = \frac{1 - V^{1-g}(x_0)}{c(g-1)} + \frac{1}{c(1-p)}. \tag{48}$$

In addition, based on the above analysis, the synchronized settling time T in (48) is ultimately bounded by

$$T = T_1 + T_2 \le \frac{1}{c(g-1)} + \frac{1}{c(1-p)}. \tag{49}$$

Case 2 ($V(x_0) < 1$): It is clear that the analytical solution takes the form

$$x = \left(\|x_0\|^{2-2p} - \vartheta_p t\right)^{\frac{1}{2-2p}} \frac{x_0}{\|x_0\|}. \tag{50}$$

The synchronized settling time in this case is

$$T = \frac{V^{1-p}(x_0)}{c(1-p)} \tag{51}$$

which is also bounded by

$$T \le \frac{1}{c(g-1)} + \frac{1}{c(1-p)} \tag{52}$$

and this completes the proof. ■

B. Time-Synchronized Control Design for Disturbed Systems

In this section, we consider the following affine system in $\mathbb{R}^n$:

$$\dot{x} = f_0(x) + g_0(x)u + \Delta \tag{53}$$

where $x = [x_1, x_2, \ldots, x_n]^T \in \mathbb{R}^n$ is the state vector, $f_0(x) \in \mathbb{R}^n$ and $g_0(x) \in \mathbb{R}^{n\times n}$ are the known parts, $u \in \mathbb{R}^n$ is the control input, and $\Delta \in \mathbb{R}^n$ represents the unknown disturbance and uncertainties.

A necessary assumption on the unknown system dynamics is made.

Assumption 1: $\dot{\Delta}$ is bounded by a known scalar δ, that is, $||\dot{\Delta}|| \leq \delta$.

In what follows, we introduce a disturbance observer to accurately estimate the unknown term Δ in finite time. Based on the disturbance observer, a time-synchronized control scheme is proposed. Then, according to the proposed Lyapunov conditions, the equilibrium of the closed-loop system (53) is proved to be time-synchronized stable.

Inspired by the multivariable super-twisting sliding-mode approach [41], we construct the following observer:

$$\dot{z}_0 = -k_1 \frac{z_0 - x}{\|z_0 - x\|^{1/2}} - k_2(z_0 - x) + f_0(x) + g_0(x)u + z_1 \tag{54}$$

$$\dot{z}_1 = -k_3 \frac{z_0 - x}{\|z_0 - x\|} - k_4(z_0 - x) \tag{55}$$

where z_0 and z_1 are used to approximate the state vector x and the unknown term Δ, respectively, and k_1, k_2, k_3, and k_4 are positive observer gains.

Defining $\tilde{z}_0 = z_0 - x$ and $\tilde{z}_1 = z_1 - \Delta$, we can further obtain the error dynamics

$$\dot{\tilde{z}}_0 = -k_1 \frac{\tilde{z}_0}{\|\tilde{z}_0\|^{1/2}} - k_2\tilde{z}_0 + \tilde{z}_1 \tag{56}$$

$$\dot{\tilde{z}}_1 = -k_3 \frac{\tilde{z}_0}{\|\tilde{z}_0\|} - k_4\tilde{z}_0 - \dot{\Delta}. \tag{57}$$

Readily following from the result in [41], we make the following assumption.

Assumption 2: $g_0(x)$ is an $n \times n$ nonsingular mapping $(\det(g_0(x)) \neq 0)$.

Assumption 2 is common in sliding-mode control results for affine systems [43]. We recall the following result for systems (56) and (57).

Lemma 7 [41]: Considering the system (56) and (57), under Assumptions 1 and 2, a range of values for k_1, k_2, k_3, and k_4 can be chosen to drive $\tilde{z}_0$ and $\tilde{z}_1$ to the origin in finite time bounded by

$$T_1 \leq \frac{2}{c} V_0^{\frac{1}{2}},\ V_0 = X_0^T P X_0 \tag{58}$$

where

$$X_0 = \left(\frac{\tilde{z}_0^T(0)}{\|\tilde{z}_0(0)\|^{1/2}}, \tilde{z}_0^T(0), \tilde{z}_1^T(0) \right)^T \tag{59}$$

$$c = \frac{2\lambda_{\max}(P)}{\lambda_{\min}(\Omega)\sqrt{\lambda_{\min}(P)}} \tag{60}$$

and $P \in \mathbb{R}^{3n\times 3n}$ and $\Omega \in \mathbb{R}^{3\times 3}$ are two positive-definite matrices.

Proof: For details, refer to [41, Proposition 1]. ■

Remark 3: The observers (54) and (55) have discontinuous right-hand sides, whose solution should be understood in the Filippov sense [44].

Remark 4: The disturbance observers (54) and (55) introduced from [41] have a multivariable super-twisting structure. In the literature, many disturbance observers and sliding-mode controllers decouples a multi-input control problem into a couple of single input control problems (e.g., [45] and [46]). This may result in discontinuities when any of the state elements changes its sign. On the contrary, the state functions (54) and (55) are continuous until $\tilde{z}_0 = 0$ is reached.

Remark 5: Note that f_0 and g_0 are considered to be known in (53). If f_0 is unknown and $\dot{f}_0$ is bounded by a known scalar, the result still holds as it can be tackled by the super-twisting observer. The problem with unknown g_0 is more challenging but not unsolvable, which is planned as a possible future direction.

Based on the disturbance observers (54) and (55), we propose a time-synchronized control law for the system (53)

$$u = -g_0^{-1}(x)\big(k_5 \mathrm{sig}_{\mathrm{n}}^{\alpha}(x) + f_0(x) + z_1\big) \tag{61}$$

where k_5 is a positive control gain, and α is defined as $0 < \alpha = \alpha_1/\alpha_2 < 1$ with positive odd integers α_1 and α_2. A block diagram of the control scheme is shown in Fig. 1.

Theorem 3: Considering system (53), if Assumptions 1 and 2 hold, under the time-synchronized control law (61) and the disturbance observers (54) and (55), the closed-loop system is time-synchronized stable, and the system state x is ratio persistent after the observer error $\tilde{z}_1$ converges to zero. The synchronized settling time is bounded by

$$T(x_0) \leq T_1 + \frac{V^{\frac{1-\alpha}{2}}(x_0)}{k_5(1-\alpha)} \tag{62}$$

where T_1 is defined in Lemma 7. When $T_1 \leq t \leq T(x_0)$, the analytical solution of the system is

$$x = \Big(\|x(T_1)\|^{1-\alpha} - k_5(1-\alpha)t\Big)^{\frac{1}{1-\alpha}} \frac{x(T_1)}{\|x(T_1)\|}. \tag{63}$$

Proof: For the system (53) under the time-synchronized control law (61), we consider a Lyapunov function

$$V = x^T x. \tag{64}$$

According to the time-synchronized control law (61), the time derivative of V reads

$$\begin{aligned} \dot{V} &= 2x^T(f_0(x) + g_0(x)u + \Delta) \\ &= 2x^T\big(-k_5 \mathrm{sig}_{\mathrm{n}}^{\alpha}(x) - z_1 + \Delta\big). \end{aligned} \tag{65}$$

In the case when $t < T_1$, based on Lemma 7, it is trivial to show that the estimation error $\tilde{z}_1$ and the closed-loop state of the system (53) are bounded. Next, for $\forall t \geq T_1$, from Lemma 7, we have $z_1 = \Delta$. Substituting the controller (61) into the system (53), we have

$$\dot{x} = -k_5 \mathrm{sig}_{\mathrm{n}}^{\alpha}(x). \tag{66}$$

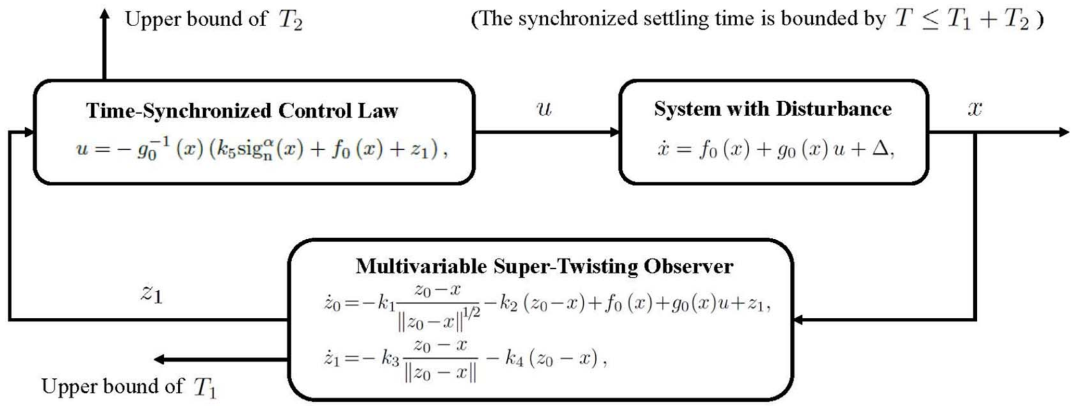

Fig. 1. Block diagram of the control scheme.

Thus, we know x is ratio persistent when $t \geq T_1$.

Furthermore, taking (66) into (65), it reads

$$\dot{V} = -2k_5 V^{\frac{\alpha+1}{2}}. \tag{67}$$

Based on Theorem 1, the closed-loop system is time-synchronized stable, with the synchronized settling time bounded by $T \leq T_1 + T_2$, where

$$T_2(x_0) = \frac{V^{\frac{1-\alpha}{2}}(x_0)}{k_5(1-\alpha)}. \tag{68}$$

In addition, according to Theorem 1, when $T_1 < t \leq T_1 + T_2$, we have the following analytical solution of the closed-loop system:

$$x = \left(\|x(T_1)\|^{1-\alpha} - k_5(1-\alpha)t\right)^{\frac{1}{1-\alpha}} \frac{x(T_1)}{\|x(T_1)\|}. \tag{69}$$

This concludes the proof. ■

C. Extension of Time-Synchronized Control

Time-synchronized control is not limited to the affine systems (53). In terms of the control design for practical systems, a TSC can be constructed on the basis of back-stepping and sliding-mode techniques.

Since Euler–Lagrange systems can be applied to characterize general mechanical systems, including robotic manipulators, autonomous vehicles, etc., the following Euler–Lagrange system is considered:

$$M(q)\ddot{q} + C(q,\dot{q})\dot{q} + g(q) = \tau(t) + \Delta \tag{70}$$

where $q \in \mathbb{R}^n$ and $\dot{q} \in \mathbb{R}^n$, respectively, denote the general position vector and velocity vector, $M(q) \in \mathbb{R}^{n\times n}$ denote the inertia matrix, $C(q,\dot{q}) \in \mathbb{R}^{n\times n}$ denote the vector of Coriolis and centrifugal matrix, $g(q) \in \mathbb{R}^n$ denote the gravitational force, and Δ denote the unknown disturbance.

We design a sliding-mode variable

$$s = \dot{q} + \gamma_1 \mathrm{sig}_{\mathrm{n}}^{p_1}(q) \tag{71}$$

where γ_1 is a positive control gain, and p_1 is a constant satisfying $0 < p_1 = p_1^*/p_2^* < 1$, with positive odd integers p_1^* and p_2^*.

For this sliding-mode design, we have the following result.

Lemma 8: The state vector q converges to the origin time-synchronously on the sliding surface (71) ($s = 0$).

Proof: On the sliding surface $s = 0$, (71) becomes

$$\dot{q} = -\gamma_1 \mathrm{sig}_{\mathrm{n}}^{p_1}(q) \tag{72}$$

and the proof can be given following that of Theorem 3. ■

For the Euler–Lagrange system (70), we design a time-synchronized sliding-mode control law

$$u = -M\big(\gamma_2 \mathrm{sig}_{\mathrm{n}}^{p_2}(s) + \rho(q,\dot{q})\big) + C(q,\dot{q})\dot{q} + g(q) - z_1 \tag{73}$$

$$\rho = \gamma_1(p_1-1)\|q\|^{p_1-3} q q^T \dot{q} + \gamma_1\|q\|^{p_2-1}\dot{q} \tag{74}$$

where γ_2 is a positive control gain, and p_2 is defined satisfying $0 < p_2 = p_3^*/p_4^* > 1$, with positive odd integers p_3^* and p_4^*. With this control, we obtain the following result for the closed-loop system.

Lemma 9: Considering the Euler–Lagrange system (70) under Assumption 1, time-synchronized control law (73), and disturbance observers (54) and (55), the closed-loop system is time-synchronized stable. After the observer error $\tilde{z}_1$ converges to zero, the sliding-mode variable s is ratio persistent, while the closed-loop system state q is ratio persistent on the sliding surface $s = 0$.

Proof: The proof can be given based on Lemma 8 and Theorem 3. Note that one should replace x by $\dot{q}$ in (54) and (55) to make the disturbance observer compatible with the Euler–Lagrange system (70). Details are omitted here. ■

Remark 6: From an application perspective, if (70) models a dual-arm robot, where $q \in \mathbb{R}^n$ contains joint information of the dual arms as in Fig. 2. According to Lemma 9, under controller (73), q is ratio persistent on the sliding surface $s = 0$, indicating that the arm joints will reach their desired values time synchronously. Furthermore, ratio persistence helps the two arms reach an object at the same time to achieve the goal of catching or grasping.

Remark 7: In Lemma 9, as a suitable extension, the time-synchronized control law (73) of the Euler–Lagrange system (70) is proposed. For an Euler–Lagrange system whose M, C, and g are not known precisely, we can separate M, C, and g as nominal parts (e.g., M_0) and uncertain parts (e.g., ΔM) as in [47]. By using disturbance observers to estimate

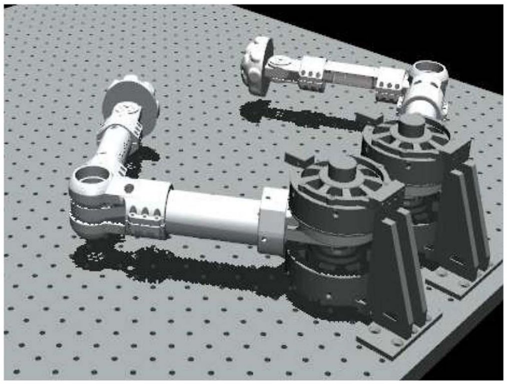

Fig. 2. Illustration of the dual-arm system.

the disturbances and uncertainties, TSC (73) is still effective. By incorporating the control design (73) into a back-stepping control framework, time-synchronized control be applied to an nth-order system. For a class of general MIMO systems that can be transformed into a regular form as in [43, eq.(5.14)], time-synchronized convergence is still achievable by slightly modifying the controller (73).

In the following two lemmas, we will continue to extend the controller (61) to the case of fixed-time synchronized control.

Lemma 10: Considering the system (53) with $\Delta = 0$, under the fixed-time-synchronized control law

$$u_{f1} = -g_0^{-1}(x)\big(k_5 \text{sig}_{\text{n}}^{p}(x) + k_6 \text{sig}_{\text{n}}^{g}(x) + f_0(x)\big) \quad (75)$$

where k_5, $k_6 > 0$, $g > 1$, and $p \in (0, 1)$, the system state x is ratio persistent, and the closed-loop system is fixed-time-synchronized stable. The synchronized settling time is bounded by

$$T(x_0) \leq \frac{1}{k_5(1-p)} + \frac{1}{k_6(g-1)}. \quad (76)$$

Proof: The proof follows from Lemma 5. ■

Next, by modifying the controller (75), the analytical solution of the fixed-time-synchronized stable system (53) is obtained.

Lemma 11: Considering the system (53) with $\Delta = 0$, under the fixed-time-synchronized control law

$$u_{f2} = -g_0^{-1}(x)\big(k_5 \text{sig}_{\text{n}}^{\eta}(x) + f_0(x)\big) \quad (77)$$

where $k_5 > 0$, $g > 1$, $p \in (0, 1)$, and

$$\eta = \begin{cases} g, & \text{if } \|x\| > 1 \\ p, & \text{if } \|x\| \leq 1 \end{cases} \quad (78)$$

the closed-loop system is fixed-time-synchronized stable. The system state x is ratio persistent. The synchronized settling time has an explicit form

$$T(x_0) = \begin{cases} \dfrac{1 - V^{\frac{1-g}{2}}(x_0)}{k_5(g-1)} + \dfrac{1}{k_5(1-p)}, & \text{if } \|x_0\| > 1 \\ \dfrac{V^{\frac{1-p}{2}}(x_0)}{k_5(1-p)}, & \text{if } \|x_0\| \leq 1. \end{cases} \quad (79)$$

The analytical solution of the closed-loop system (1) takes the form: 1) in the case of $\|x_0\| > 1$

$$x = \begin{cases} \left(\|x_0\|^{1-g} - \vartheta_g t\right)^{\frac{1}{1-g}} \dfrac{x_0}{\|x_0\|}, & \text{if } t < T_1 \\ \left(k_5^{\frac{p-1}{2}} - \vartheta_p (t - T_1)\right)^{\frac{1}{1-p}} \dfrac{x_0}{\|x_0\|}, & \text{if } t \geq T_1 \end{cases} \quad (80)$$

and 2) in the case of $\|x_0\| \leq 1$

$$x = \left(\|x_0\|^{1-p} - \vartheta_p t\right)^{\frac{1}{1-p}} \frac{x_0}{\|x_0\|} \quad (81)$$

where $T_1 = (1 - V^{(1-g/2)}(x_0))/(k_5(g-1))$, $\vartheta_p = k_5(1-p)$, and $\vartheta_g = k_5(1-g)$.

Proof: Considering a Lyapunov function $V = x^T x$ and analyzing its time derivative, the proof is then readily derived from Theorem 2. ■

Remark 8: Despite the switching power η, it can be observed that the fixed-time synchronized control law (77) is continuous by verifying the controller (77) at the point $\|x\| = 1$.

Remark 9: Note that the system (53) without disturbances and uncertainties (i.e., $\Delta = 0$) is considered in Lemmas 10 and 11. The reason is that if we directly use the disturbance observers (54) and (55) to estimate the unknown term Δ, the achieved result in Lemmas 10 and 11 will become time-synchronized stability rather than the fixed one, since the disturbance observers (54) and (55) converge in finite time. One can replace the finite-time disturbance observers (54) and (55) by the fixed-time ones to achieve the fixed-time-synchronized stable result for the system (53) under disturbances and uncertainties, for example, the state estimation approaches in [46] and [48], to name a few.

IV. Illustrative Examples

A. Case 1 (Comparison With Finite-Time Control)

In this section, we examine TSC (61) to show the properties of time-synchronized stability. Consider the plant (53) with functions $f_0 = 3x$ and $g_0 = I_3$, disturbance $\Delta = [2, 3\sin(0.02\pi t), 4\sin(0.05\pi t + \pi/2)]^T$, and initial state $x_0 = [2, -7, 10]^T$. In what follows, to yield a comprehensive comparison, we introduce a typical finite-time controller (FTC).

Define a classical sign function

$$\text{sig}_{\text{c}}^{\alpha}(x) = \left[\text{sign}_{\text{c}}(x_1)|x_1|^{\alpha}, \ldots, \text{sign}_{\text{c}}(x_n)|x_n|^{\alpha}\right]^T \quad (82)$$

where

$$\text{sign}_{\text{c}}(x_i) \triangleq \begin{cases} +1, & x_i > 0 \\ 0, & x_i = 0 \\ -1, & x_i < 0 \end{cases} \quad (83)$$

with $x = [x_1, x_2, \ldots, x_n]^T$.

Using the sign function (82), we can design an FTC.

Lemma 12: For system (53), under the following finite-time control law:

$$\overline{u} = -g_0^{-1}(x)\big(k_5 \text{sig}_{\text{c}}^{\alpha}(x) + f_0(x) + z_1\big) \quad (84)$$

TABLE I
PARAMETERS FOR SIMULATION: CASE 1

Parameters	Values	Parameters	Values
k_1	10	k_2	50
k_3	10	k_4	20
k_5	0.5	α	7/11

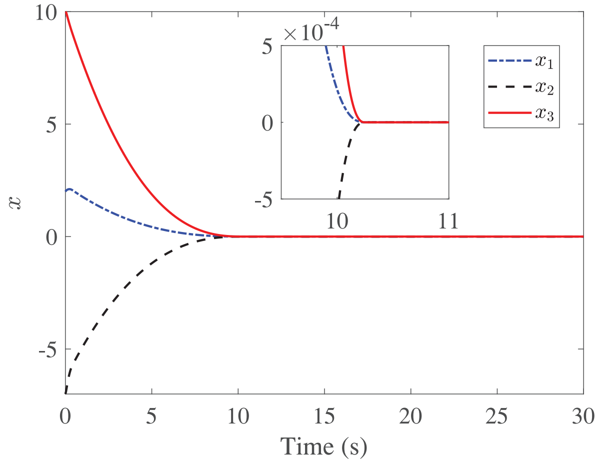

Fig. 3. System state x under the time-synchronized control law (61).

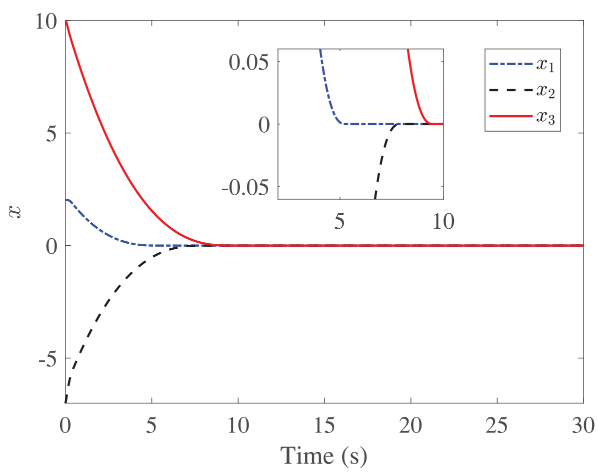

Fig. 4. System state x under the finite-time control law (84).

and the disturbance observers (54) and (55), the closed-loop system is finite-time stable.

Proof: The proof is clear by Lemma 1. ∎

Simulation parameters are shown in Table I, where the TSC and FTC share the same control and observer parameters to produce a fair comparison.

As presented in Figs. 3 and 4, under the time-synchronized control law (61), all the system state elements reach the equilibrium at the same time, while under the finite-time law (84), three state elements arrive at the equilibrium at different times. Moreover, in Fig. 3, the state elements converge time synchronously even when we zoom in at the level of $\times 10^{-4}$.

The property of ratio persistence is shown in Fig. 5. It evidently approves declared time-synchronized stability under the controller (61), where after T_1, the ratio of each pair of the

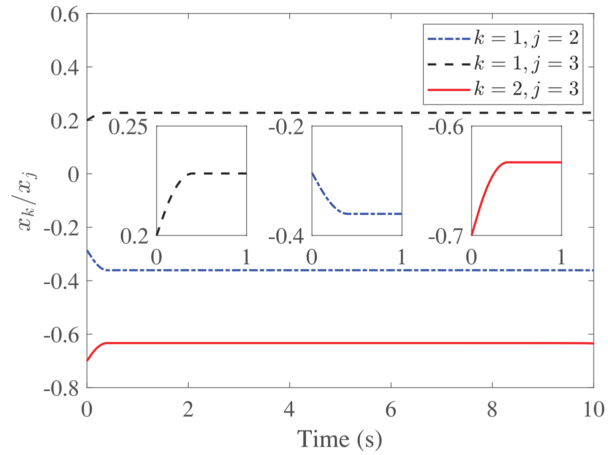

Fig. 5. Ratio of each pair of the state elements.

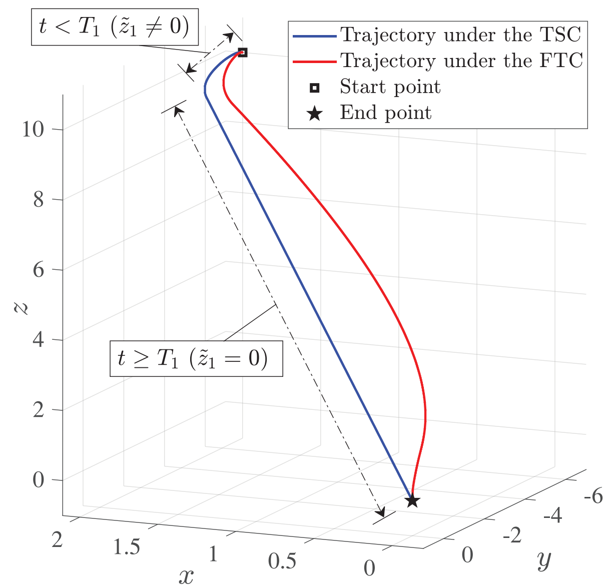

Fig. 6. Trajectories of x under TSC and FTC. (It can be observed that the trajectory of x governed by the TSC is the shortest path in the 3-D space when $t \geq T_1$.)

state elements is time invariant. Specific subfigures are also included to showcase how the ratio converges to a constant.

The 3-D state trajectories under the time-synchronized control law (61) and finite-time law (84) are presented in Fig. 6. The trajectory under the time-synchronized control law (61) (the blue curve) is divided into two parts: 1) the trajectory s.t. $t < T_1$ and 2) the trajectory s.t. $t \geq T_1$. It is noted that the trajectory s.t. $t < T_1$ is a curve since the estimation from the disturbance observers (54) and (55) is not accurate, that is, $\tilde{z}_1 \neq 0$. Given a precise disturbance estimation, it suggests that time-synchronized stability helps the system generate a smoother and shorter path. As according to Theorem 3, when $\tilde{z}_1 = 0$, $t \geq T_1$, the output trajectory of the closed-loop system under the time-synchronized control law (61) is ratio persistent, being a straight line in the 3-D space. On the contrary, the trajectory governed by the finite-time law (84) (the red curve) is much longer.

From Fig. 7, the disturbance observers (54) and (55) yields an accurate estimation for both controllers (61) and (84) within

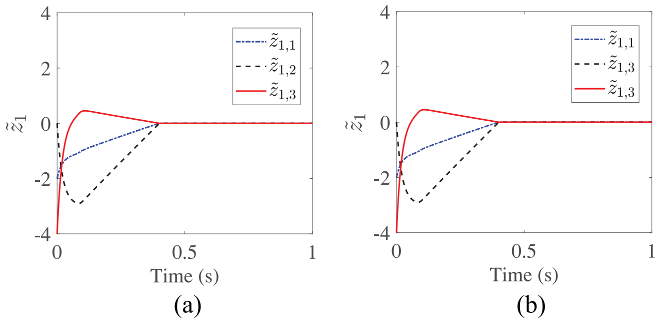

Fig. 7. Estimation errors $\tilde{z}_1$. (a) Under the time-synchronized control law (61). (b) Under the finite-time control law (84).

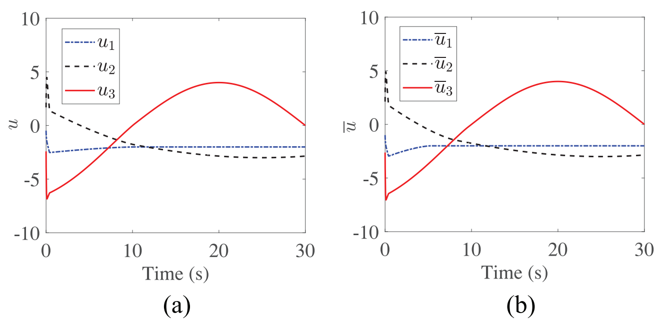

Fig. 8. Control inputs: (a) of the time-synchronized control law u; and (b) of the finite-time control law $\bar{u}$.

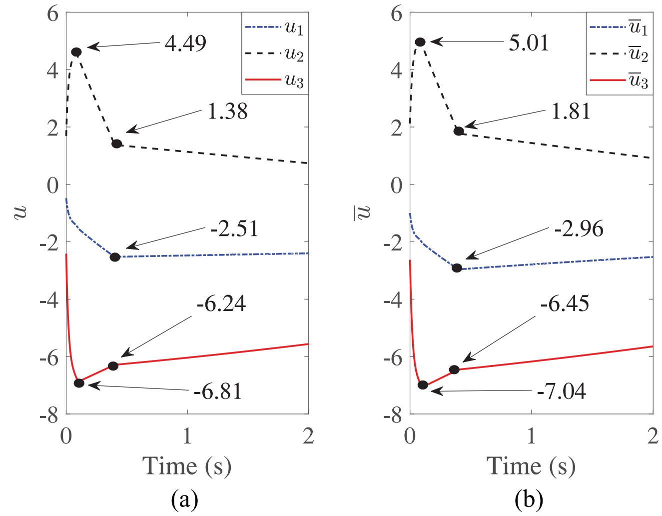

Fig. 9. Control inputs with detailed values: (a) of the time-synchronized control law u and (b) of the finite-time control law $\bar{u}$. (The values with arrows denote $|u_i|$ or $|\bar{u}_i|$, $i = 1, 2, 3$ at black solid points.)

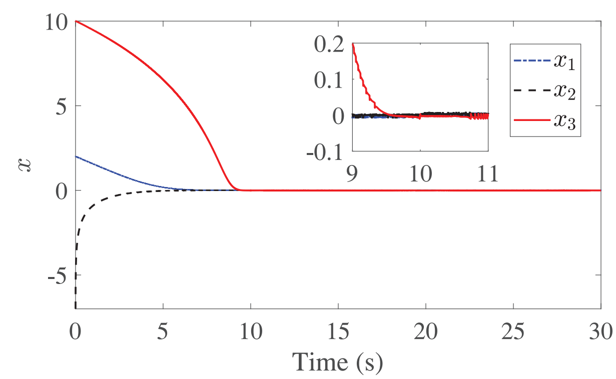

Fig. 10. System state x under the prescribed-time control law (85).

0.5 s ($T_1 < 0.5$ s). Note that the elements of the estimation error in Fig. 7 seem to arrive at the origin at the same time. That is, because, the error dynamics (56) is ratio persistent given $\tilde{z}_1 = 0$ (which is certainly achieved in finite time), while the rigorous proof of its "time-synchronized-like behavior" is beyond the scope of this approach. As mentioned, the ratio persistence widely exists in the literature of control system design, which grants the proposed result wide applicability. The relevant control inputs are shown in Fig. 8, while it seems that no significant difference can be observed between the two controllers. Furthermore, the detailed initial values of the control inputs are provided in Fig. 9. It is clear that the FTC requires a larger control input compared with TSC. This explains why compared with TSC, FTC seems to achieve a faster convergence rate as in Figs. 3 and 4. The control inputs in Fig. 8 still have huge fluctuation after T_1 since the controllers need to neutralize the external disturbance Δ. This validates the effectiveness of the controllers and disturbance observers.

B. Case 2 (Comparison With Prescribed-Time Control)

Prescribed-time control forces the system state to converge to the origin before or at a given prespecified time instant. One may wonder whether time-synchronized convergence can be achieved by designing prescribed-time controllers (PTCs) for each subsystem, and how this approach is different from the prescribed-time control.

To fully showcase the differences compared with prescribed-time control, considering the plant (53) (the system parameters f_0 and g_0, and the disturbance Δ are the same as those in Section IV-A for fairness of comparison), we would like to introduce the following PTC that is proposed in the very recent literature [28] and is also analyzed in the state-of-the-art work [27]:

$$\bar{u}_i = u_{ni} - \kappa_2 \mathrm{sign_c}(s_i) - 3x_i \tag{85}$$

$$u_{ni} = \begin{cases} \dfrac{-\kappa_1(e^{x_i} - 1)}{e^{x_i}\left(t_f - t\right)}, & \text{if } 0 \le t < t_f \\ 0, & \text{otherwise} \end{cases} \tag{86}$$

$$s_i = x_i - x_i(0) - \int_0^t u_{ni} d\tau \tag{87}$$

where $i = 1, 2, 3$, κ_1, κ_2 are positive control gains, and t_f is the prescribed settling time. The basic idea behind this design lies in that $u_{ni} \to \infty$ as $t \to t_f$, which guarantees the convergence at the predefined time instant t_f. The detailed proof follows from the results in [28].

The simulation parameters for the controller (85) are selected as $\kappa_1 = 5$, $\kappa_2 = 4$, and $t_f = 10$. Fig. 10 shows that all the system state elements converge to the origin before $t = 10$ s. In Fig. 11, the control input $\bar{u}$ is provided. The state trajectories under the time-synchronized control law (61) and predefined-time law (85) are given in Fig. 12. Given a precise disturbance estimation, it suggests that the TSC helps the system yield a smoother and shorter path. In accordance with

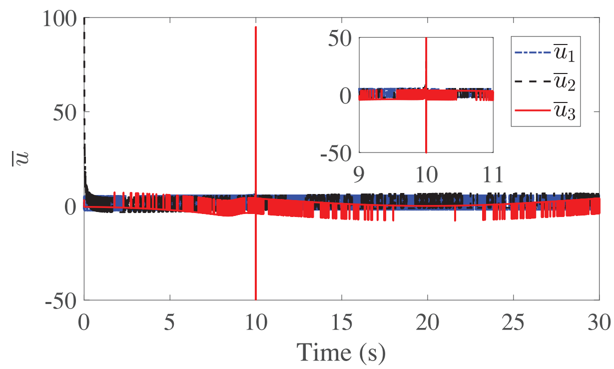

Fig. 11. Control input $\bar{u}$ of the prescribed-time control law (85).

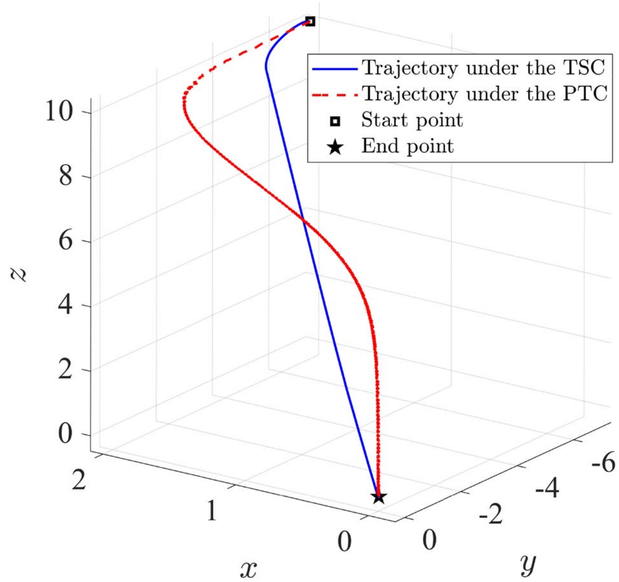

Fig. 12. Trajectories of x under the TSC and under the PTC. (It can be observed that the trajectory of x governed by TSC is the shortest path in the 3-D space after accurate disturbance estimation is acquired by the disturbance observer.)

Theorem 3, when $\tilde{z}_1 = 0$, $t \geq T_1$, the system output under the time-synchronized control law (61) is ratio persistent, which is a straight line. In contrast, the trajectory governed by the prescribed-time control law (85) is longer. In summary, we note the following facts (note that the comparison is conducted under the same initial state and disturbance).

1) For PTC (85), despite the same prescribed settling time t_f is chosen for each subsystem, some state elements may still converge to the origin faster or slower due to the variance of the parameter selection and the initial state. In this case, during the convergence, some state elements may be significantly close to the origin while the others are still far from the origin (see Fig. 10). On the contrary, TSC (61) guarantees the same convergence time while preserving the ratio of the state elements (see Fig. 3).
2) To cancel the disturbances, the chattering behavior is inevitable in PTC (85) (see Fig. 11).
3) When $t \to t_f$, the control input of the prescribed-time (85) may be relevant large (see the peak in Fig. 11).

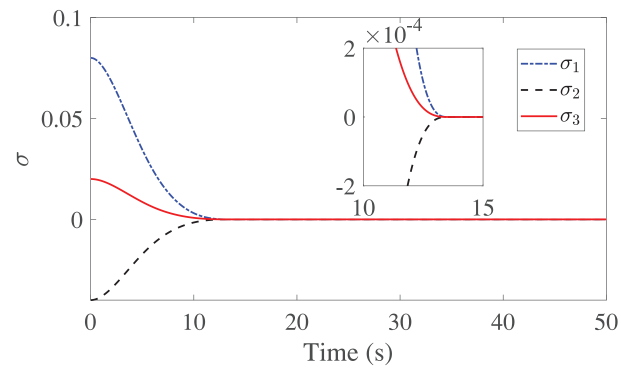

Fig. 13. Spacecraft attitude σ under TSC (73).

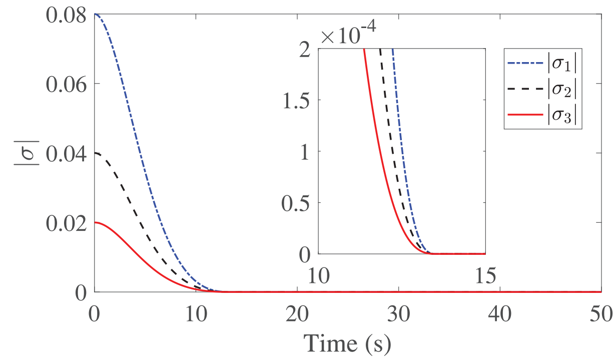

Fig. 14. Norm of the spacecraft attitude σ under the time-synchronized control law (73).

4) TSC (61) yields a shorter and smoother trajectory due to the property of ratio persistence (see Fig. 12).
5) PTC (85) strictly ensures the convergence before a predefined settling time t_f while the PTC (85) does not.

The above observation and discussion are also in line with the analysis and simulation in [28]. Actually, the PTCs in [28] and [27] hold the merit, which guarantees the convergence before/at a predefined settling time t_f that explicitly integrated in the controller. In conclusion, prescribed-time control and time-synchronized control have different focuses and their respective advantages.

Therefore, interesting possible future directions may include time-synchronized control with predefined/prescribed settling time.

C. Case 3 (Time-Synchronized Control For Euler–Lagrange Systems)

In this section, simulation results for practical Euler–Lagrange systems are provided to further verify the effectiveness.

We consider the spacecraft attitude dynamics as follows:

$$M(\sigma)\ddot{\sigma} + C(\sigma, \dot{\sigma})\dot{\sigma} = u(t) \qquad (88)$$

where σ are the modified Rodrigues parameters [49]. The system model (88) and its parameters are the same as those in [50], where the inertia matrix is

$$[11, 0.3, 0.2; 0.4, 9, 0.5; 0.2, 0.4, 8] \left(\mathrm{kg} \cdot \mathrm{m}^2\right). \qquad (89)$$

TABLE II
PARAMETERS FOR SIMULATION: CASE 3

Parameters	Values	Parameters	Values
γ_1	0.1	γ_2	0.1
p_2	$7/11$	p_2	$7/11$
k_1	10	k_2	50
k_3	10	k_4	20
$\sigma(0)$	$[0.08, -0.04, 0.02]^T$		
Δ	$[0.05, 0.03\sin(0.02\pi t), 0.04\sin(0.05\pi t + \pi/2)]^T$		

Other simulation parameters for the controller (73) are given in Table II.

The following simulation results are provided to fully verify the performance. In Figs. 13 and 14, both the system state and its norm are presented for clarity, where all the state elements arrive at the origin synchronously. This approves the claimed time-synchronized convergence property.

V. CONCLUSION

In this article, general Lyapunov-like theorems of (fixed-) time-synchronized stability are proposed, where the analytical solutions of (fixed-) time-synchronized stable system dynamics are derived. For a class of multivariable systems under external disturbances and model uncertainties, a robust time-synchronized control law has been proposed. Furthermore, extensions to other system dynamics are suitably discussed.

REFERENCES

[1] S. Yu, X. Yu, B. Shirinzadeh, and Z. Man, "Continuous finite-time control for robotic manipulators with terminal sliding mode," *Automatica*, vol. 41, no. 11, pp. 1957–1964, 2005.

[2] M. Galicki, "Finite-time control of robotic manipulators," *Automatica*, vol. 51, pp. 49–54, Jan. 2015.

[3] C. Yang, Y. Jiang, W. He, J. Na, Z. Li, and B. Xu, "Adaptive parameter estimation and control design for robot manipulators with finite-time convergence," *IEEE Trans. Ind. Electron.*, vol. 65, no. 10, pp. 8112–8123, Oct. 2018.

[4] Y. Hong, Y. Xu, and J. Huang, "Finite-time control for robot manipulators," *Syst. Control Lett.*, vol. 46, no. 4, pp. 243–253, 2002.

[5] L. Wang, T. Chai, and L. Zhai, "Neural-network-based terminal sliding-mode control of robotic manipulators including actuator dynamics," *IEEE Trans. Ind. Electron.*, vol. 56, no. 9, pp. 3296–3304, Sep. 2009.

[6] H. Du, S. Li, and C. Qian, "Finite-time attitude tracking control of spacecraft with application to attitude synchronization," *IEEE Trans. Autom. Control*, vol. 56, no. 11, pp. 2711–2717, Nov. 2011.

[7] B. Xiao, Q. Hu, and Y. Zhang, "Adaptive sliding mode fault tolerant attitude tracking control for flexible spacecraft under actuator saturation," *IEEE Trans. Control Syst. Technol.*, vol. 20, no. 6, pp. 1605–1612, Nov. 2012.

[8] A.-M. Zou, K. D. Kumar, Z.-G. Hou, and X. Liu, "Finite-time attitude tracking control for spacecraft using terminal sliding mode and Chebyshev neural network," *IEEE Trans. Syst., Man, Cybern. B, Cybern.*, vol. 41, no. 4, pp. 950–963, Aug. 2011.

[9] R. Engel and G. Kreisselmeier, "A continuous-time observer which converges in finite time," *IEEE Trans. Autom. Control*, vol. 47, no. 7, pp. 1202–1204, Jul. 2002.

[10] F. J. Bejarano and L. Fridman, "High order sliding mode observer for linear systems with unbounded unknown inputs," *Int. J. Control*, vol. 83, no. 9, pp. 1920–1929, 2010.

[11] W. Perruquetti, T. Floquet, and E. Moulay, "Finite-time observers: Application to secure communication," *IEEE Trans. Autom. Control*, vol. 53, no. 1, pp. 356–360, Feb. 2008.

[12] Y. Zhao, Y. Liu, G. Wen, W. Ren, and G. Chen, "Edge-based finite-time protocol analysis with final consensus value and settling time estimations," *IEEE Trans. Cybern.*, vol. 50, no. 4, pp. 1450–1459, Apr. 2020.

[13] S. Khoo, L. Xie, and Z. Man, "Robust finite-time consensus tracking algorithm for multirobot systems," *IEEE/ASME Trans. Mechatron.*, vol. 14, no. 2, pp. 219–228, Apr. 2009.

[14] Y. Cao and W. Ren, "Finite-time consensus for multi-agent networks with unknown inherent nonlinear dynamics," *Automatica*, vol. 50, no. 10, pp. 2648–2656, 2014.

[15] F. Xiao, L. Wang, J. Chen, and Y. Gao, "Finite-time formation control for multi-agent systems," *Automatica*, vol. 45, no. 11, pp. 2605–2611, 2009.

[16] D. Li, S. S. Ge, W. He, G. Ma, and L. Xie, "Multilayer formation control of multi-agent systems," *Automatica*, vol. 109, Nov. 2019, Art. no. 108558.

[17] Z. Meng, W. Ren, and Z. You, "Distributed finite-time attitude containment control for multiple rigid bodies," *Automatica*, vol. 46, no. 12, pp. 2092–2099, 2010.

[18] Y. Cao, W. Ren, and Z. Meng, "Decentralized finite-time sliding mode estimators and their applications in decentralized finite-time formation tracking," *Syst. Control Lett.*, vol. 59, no. 9, pp. 522–529, 2010.

[19] X. Wang, S. Li, and P. Shi, "Distributed finite-time containment control for double-integrator multiagent systems," *IEEE Trans. Cybern.*, vol. 44, no. 9, pp. 1518–1528, Sep. 2014.

[20] Y. Li, L. Liu, and G. Feng, "Adaptive finite-time controller design for T–S fuzzy systems," *IEEE Trans. Cybern.*, vol. 47, no. 9, pp. 2425–2436, Sep. 2017.

[21] J. Wang, S. Ma, C. Zhang, and M. Fu, "Finite-time H_∞ filtering for nonlinear singular systems with nonhomogeneous Markov jumps," *IEEE Trans. Cybern.*, vol. 49, no. 6, pp. 2133–2143, Jun. 2019.

[22] Y. Sheng, F. L. Lewis, Z. Zeng, and T. Huang, "Lagrange stability and finite-time stabilization of fuzzy memristive neural networks with hybrid time-varying delays," *IEEE Trans. Cybern.*, vol. 50, no. 7, pp. 2959–2970, Jul. 2020.

[23] V. T. Haimo, "Finite time controllers," *SIAM J. Control Optim.*, vol. 24, no. 4, pp. 760–770, 1986.

[24] S. P. Bhat and D. S. Bernstein, "Finite-time stability of continuous autonomous systems," *SIAM J. Control Optim.*, vol. 38, no. 3, pp. 751–766, 2000.

[25] A. Polyakov, "Nonlinear feedback design for fixed-time stabilization of linear control systems," *IEEE Trans. Autom. Control*, vol. 57, no. 8, pp. 2106–2110, Aug. 2012.

[26] E. Cruz-Zavala, J. A. Moreno, and L. M. Fridman, "Uniform robust exact differentiator," *IEEE Trans. Autom. Control*, vol. 56, no. 11, pp. 2727–2733, Nov. 2011.

[27] B. Zhou, "Finite-time stability analysis and stabilization by bounded linear time-varying feedback," *Automatica*, vol. 121, Nov. 2020, Art. no. 109191.

[28] A. K. Pal, S. Kamal, S. K. Nagar, B. Bandyopadhyay, and L. Fridman, "Design of controllers with arbitrary convergence time," *Automatica*, vol. 112, Feb. 2020, Art. no. 108710.

[29] I.-S. Jeon, J.-I. Lee, and M.-J. Tahk, "Homing guidance law for cooperative attack of multiple missiles," *J. Guid. Control Dyn.*, vol. 33, no. 1, pp. 275–280, 2010.

[30] J. Zhou, J. Yang, and Z. Li, "Simultaneous attack of a stationary target using multiple missiles: A consensus-based approach," *Sci. China Inf. Sci.*, vol. 60, no. 7, pp. 1–14, 2017.

[31] J. Zhou and J. Yang, "Distributed guidance law design for cooperative simultaneous attacks with multiple missiles," *J. Guid. Control Dyn.*, vol. 39, no. 10, pp. 2436–2444, 2016.

[32] T. Lyu, Y. Guo, C. Li, G. Ma, and H. Zhang, "Multiple missiles cooperative guidance with simultaneous attack requirement under directed topologies," *Aerosp. Sci. Technol.*, vol. 89, pp. 100–110, Jun. 2019.

[33] D. Li, H. Yu, K. P. Tee, Y. Wu, S. S. Ge, and T. H. Lee, "On time-synchronized stability and control," *IEEE Trans. Syst., Man, Cybern.*, early access, Jan. 29, 2021, doi: 10.1109/TSMC.2021.3050183.

[34] C. Edwards and S. Spurgeon, *Sliding Mode Control: Theory and Applications*. Boca Raton, FL, USA: CRC, 1998.

[35] M. T. Hamayun, C. Edwards, and H. Alwi, "Design and analysis of an integral sliding mode fault-tolerant control scheme," *IEEE Trans. Autom. Control*, vol. 57, no. 7, pp. 1783–1789, Jul. 2012.

[36] A. K. Sanyal and J. Bohn, "Finite-time stabilisation of simple mechanical systems using continuous feedback," *Int. J. Control*, vol. 88, no. 4, pp. 783–791, 2015.

[37] V. Utkin, J. Guldner, and J. Shi, *Sliding Mode Control in Electro-Mechanical Systems*. Boca Raton, FL, USA: CRC, 2009.

[38] S. Gutman, "Uncertain dynamical systems—A Lyapunov min–max approach," *IEEE Trans. Autom. Control*, vol. AC-24, no. 3, pp. 437–443, Jun. 1979.

[39] A. Levant and B. Shustin, "Quasi-continuous MIMO sliding-mode control," *IEEE Trans. Autom. Control*, vol. 63, no. 9, pp. 3068–3074, Sep. 2018.
[40] D. Li, S. S. Ge, and T. H. Lee, "Fixed-time-synchronized consensus control of multi-agent systems," *IEEE Trans. Control Netw. Syst.*, early access, Oct. 28, 2020, doi: 10.1109/TCNS.2020.3034523.
[41] I. Nagesh and C. Edwards, "A multivariable super-twisting sliding mode approach," *Automatica*, vol. 50, no. 3, pp. 984–988, 2014.
[42] J. A. Moreno and M. Osorio, "Strict Lyapunov functions for the super-twisting algorithm," *IEEE Trans. Autom. Control*, vol. 57, no. 4, pp. 1035–1040, Apr. 2012.
[43] R. A. Decarlo, S. H. Zak, and G. P. Matthews, "Variable structure control of nonlinear multivariable systems: A tutorial," *Proc. IEEE*, vol. 76, no. 3, pp. 212–232, Mar. 1988.
[44] A. F. Filippov, *Differential Equations with Discontinuous Right-Hand Side*. Dordrecht, The Netherlands: Kluwer, 1988.
[45] B. Li, Q. Hu, Y. Yang, and O. A. Postolache, "Finite-time disturbance observer based integral sliding mode control for attitude stabilisation under actuator failure," *IET Control Theory Appl.*, vol. 13, no. 1, pp. 50–58, Jan. 2019.
[46] M. Basin, P. Rodriguez-Ramirez, and A. Garza-Alonso, "Continuous fixed-time convergent super-twisting algorithm in case of unknown state and disturbance initial conditions," *Asian J. Control*, vol. 21, no. 1, pp. 323–338, 2019.
[47] Z. Li, C.-Y. Su, L. Wang, Z. Chen, and T. Chai, "Nonlinear disturbance observer-based control design for a robotic exoskeleton incorporating fuzzy approximation," *IEEE Trans. Ind. Electron.*, vol. 62, no. 9, pp. 5763–5775, Sep. 2016.
[48] M. Basin, C. B. Panathula, and Y. Shtessel, "Multivariable continuous fixed-time second-order sliding mode control: Design and convergence time estimation," *IET Control Theory Appl.*, vol. 11, no. 8, pp. 1104–1111, May 2017.
[49] J. Ahmed, V. T. Coppola, and D. S. Bernstein, "Adaptive asymptotic tracking of spacecraft attitude motion with inertia matrix identification," *J. Guid. Control Dyn.*, vol. 21, no. 5, pp. 684–691, 1998.
[50] D. Li, G. Ma, C. Li, W. He, J. Mei, and S. S. Ge, "Distributed attitude coordinated control of multiple spacecraft with attitude constraints," *IEEE Trans. Aerosp. Electron. Syst.*, vol. 54, no. 5, pp. 2233–2245, Oct. 2018.

Dongyu Li (Member, IEEE) received the B.S. and Ph.D. degrees from Control Science and Engineering, Harbin Institute of Technology, China, in 2016 and 2020. He was a joint Ph.D. student with the Department of Electrical and Computer Engineering, National University of Singapore from 2017 to 2019, and a research fellow with the Department of Biomedical Engineering, National University of Singapore, from 2019 to 2021. He is currently an Associate Professor with the School of Cyber Science and Technology, Beihang University, China. His research interests include networked system cooperation, adaptive systems, and robotic control.

Keng Peng Tee (Member, IEEE) received the B.Eng. (First Class Hons.), M.Eng., and Ph.D. degrees from the National University of Singapore, Singapore, in 2001, 2003, and 2008, respectively.

He is currently a Senior Scientist with A*STAR's Institute for Infocomm Research, Singapore, where he holds an appointment as the Head of the Manipulation Unit, Robotics Department. His active research interests include manipulation learning, adaptive systems, and human–robot collaboration.

Lihua Xie (Fellow, IEEE) received the Ph.D. degree in electrical engineering from the University of Newcastle, Callaghan, NSW, Australia, in 1992.

Since 1992, he has been with the School of Electrical and Electronic Engineering, Nanyang Technological University, Singapore, where he is currently a Professor and the Director of Delta–NTU Corporate Laboratory for Cyber-Physical Systems. He served as the Head of the Division of Control and Instrumentation from 2011 to 2014. He held teaching appointments with the Department of Automatic Control, Nanjing University of Science and Technology, Nanjing, China, from 1986 to 1989. His research interests include robust control and estimation, networked control systems, multiagent networks, localization, and unmanned systems.

Prof. Xie is the Editor-in-Chief of *Unmanned Systems* and an Associate Editor for IEEE Transactions on Network Control Systems. He served as an Editor of IET Book Series in Control and an Associate Editor of a number of journals, including IEEE Transactions on Automatic Control, *Automatica*, IEEE Transactions on Control Systems Technology, and IEEE Transactions on Circuits and Systems—II: Express Briefs. He was an IEEE Distinguished Lecturer from 2012 to 2014 and an Elected Member of the Board of Governors, IEEE Control System Society from 2016 to 2018. He is a Fellow of the Academy of Engineering Singapore, IFAC, and CAA.

Haoyong Yu (Senior Member, IEEE) received the B.S. and M.S. degrees in mechanical engineering from Shanghai Jiao Tong University, Shanghai, China, in 1988 and 1991, respectively, and the Ph.D. degree in mechanical engineering from the Massachusetts Institute of Technology, Cambridge, MA, USA, in 2002.

He is currently an Associate Professor with the Department of Biomedical Engineering, National University of Singapore, Singapore. His areas of research include medical robotics, rehabilitation engineering and assistive technologies, system dynamics, and control.